International Journal of Fluid Machinery and Systems
Vol. 1, No. 1, October-December 2008

Original Paper

Influence of Blade Profiles on Flow around Wells Turbine

Masami Suzuki and Chuichi Arakawa

Department of Mechanical Engineering, Graduate School of Engineering, The University of Tokyo
7-3-1 Hongo, Bunkyo-ku, Tokyo, 113-8656 Japan

Abstract

The Wells turbine rotor consists of several symmetric airfoil blades arranged around a central hub, and the stagger angle is 90 degrees. These characteristics simplify the total construction of OWC type wave energy converters. Although the Wells turbine is simple, the turbine produces a complicated flow field due to the peculiar arrangement of blades, which can rotate in the same direction irrespective of the oscillating airflow. In order to understand these flows, flow visualization is carried out with an oil-film method in the water tunnel. This research aims to analyze the mechanism of the 3-D flows around the turbine with the flow visualization. The flow visualization explained the influence of attack angle, the difference between fan-shaped and rectangular wings, and the sweep angle.

Keywords: Wells Turbine, Flow Visualization, Oil Film Method, Wave Power Generation, Ocean Engineering

1. Introduction

A wave-power-generating system of Oscillating Water Column (OWC) type is composed of a turbine-generator and an air chamber in which OWC converts wave energy into oscillating airflow [1]~[2]. The wave energy is absorbed by the air chamber fixed or floating at the sea surface. A Wells turbine is used for the air turbine because it is suitable for the operation in oscillating airflow. The basic feature of the Wells turbine is that even though the cyclic airflow produces oscillating axial forces on the airfoil blades, the tangential force on the rotor is always in the same direction. This induces the rotation of the rotor and produces a power output without the need for the sophisticated rectifying valves. The turbine rotor consists of several symmetric airfoil blades arranged around a central hub, and the stagger angle is 90 degrees. These characteristics simplify construction of OWC type wave energy converters. The characteristics became clear by the performance tests, which were done in the wind tunnel [3] ~ [6]. The 3-D Navier-Stokes equations were solved numerically to predict the characteristics of a Wells turbine with computational fluid dynamics (CFD) codes including commercial ones [7]. But they did not cover the stall condition and detailed simulation of the performance.

In order to understand the flow field, the authors visualize it by using an oil film method in the water tunnel and an in house CFD code [8]. This research aims to analyze the mechanism of the 3-D flows around the turbine with the flow visualization.

2. Experimental Apparatus

2.1 Performance Test

Figure 1 is a schematic view of the experimental apparatus. The inside diameter of the casing $D_c=2R_c$ is 304.4mm, and the hub diameter $D_h=2R_h$ is 215mm. Figure 2 describes four rotors which have a tip clearance of 1.0mm. Fig.2a shows a rotor which has 8 rectangular blades, a chord length of 73.5mm, a NACA 0021 wing section, and a solidity of 0.7 at the root mean square of the radius, $R_{RMS}=\sqrt{(R_t^2+R_h^2)/2}$. Figures 2b~d show rotors which have 7 fan-shaped blades, a chord length of 95.0mm at the

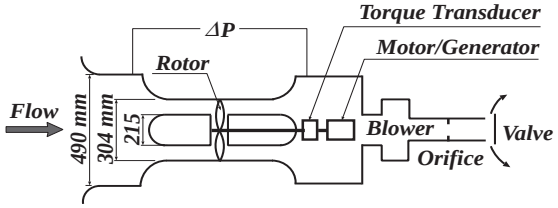

Fig. 1 Schematic explanation of experimental apparatus for performance test

Received July 4 2008; revised November 12 2008; accepted for publication November 13 2008: Review conducted by Prof. Wang Le-qing. (Paper number O08014)
Corresponding author: Masami Suzuki, Assistant Professor, wells@cfdl.t.u-tokyo.ac.jp

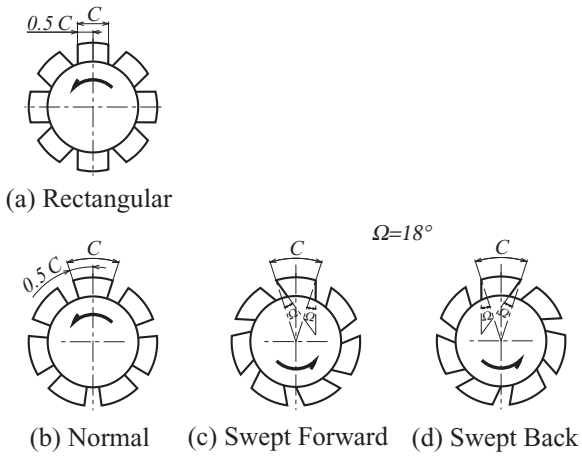

(a) Rectangular (b) Normal (c) Swept Forward (d) Swept Back

Fig. 2 Profiles of rotors

tip, and a solidity of 0.7. The wing section is NACA 0012 at the tip, and the same thickness from the hub to the tip. Figures 2b, 2c, and 2d show the rotors with the normal, the swept forward, and the swept back blades, respectively. The sweep angle is 18 degrees for the swept forward and swept back blades. Most of the investigations on Wells turbine were conducted with rotors consisting of airfoil blades of rectangular planform because of the stronger structure for the centrifugal force than the fan-shaped one. On the other hand, the turbine with the fan-shaped blades is able to obtain the high efficiency.

The wind tunnel in Fig.1 is of suction type. The measured data are the pressure drop across the turbine, the turbine torque, the rotational speed and the flow rate. The Reynolds number is described with the representative velocity and length, which are assigned the relative velocity at the tip, $\sqrt{U^2+V_a{}^2}$, and the blade's chord length, respectively. U, V_a and α are the blade speed of the tip, the space average axial velocity and the angle of attack, respectively. The Reynolds numbers of the rectangular blade are 1.7×10^5 at α=0º, 1.6×10^5 at α=15º, and 1.2×10^5 at α=19º, respectively. The Reynolds numbers of the fan-shaped blades are 2.2×10^5 at α=0º, 2.0×10^5 at α=15º, and 1.2×10^5 at α=19º, respectively.

2.2 Flow Visualization

Figure 3 is an overall view of circulating-water tunnel in which the flow around the Wells turbine can be visualized with flow visualization techniques. The size of this apparatus and the Reynolds number are the same as for the wind tunnel in the above performance test. The flow visualization technique used in this water tunnel is the oil-film method. The test section is covered with the transparent acrylic casing (2) so that the inner flow can be observed. The pump (3) sucks the water from the upstream tank (1) through the turbine (5), the orifice (7) and the flow control valve (6), and it discharges to the upstream tank.

The oil film method uses Titanium dioxide, Liquid paraffin and Oleic acid which are mixed with a ratio of 10:5:6 by weight. The rotational speed is 200rpm when the angle of attack is less than 14.5º, while the axial velocity is approximately 0.8 m/sec when the angle of attack is larger than 14.5º.

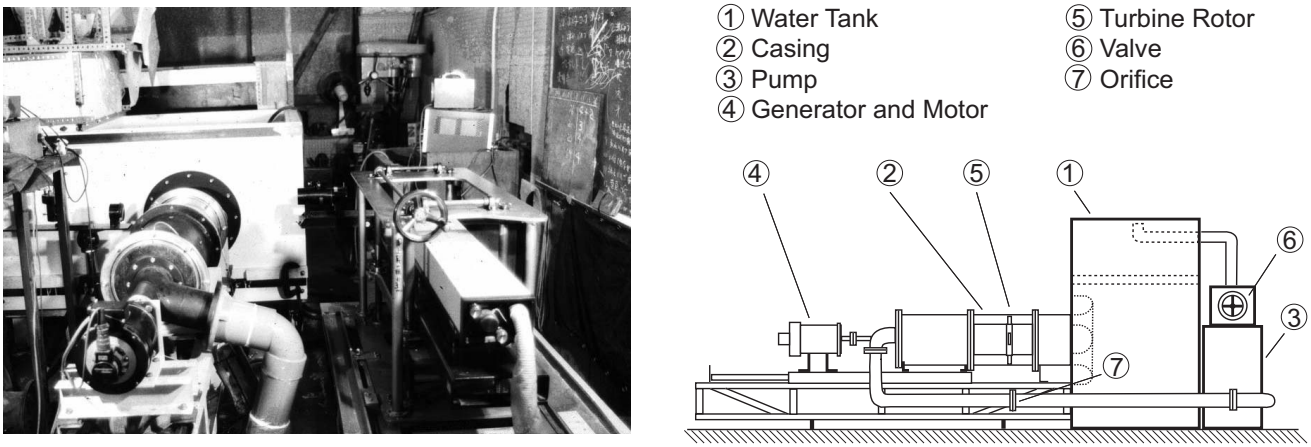

Fig. 3 Experimental apparatus for flow visualization

3. Experimental Results And Discussion

3.1 Performance of turbine

Figures 4 ~ 5 show the results of the performance test for the Wells turbine. The nondimensional factors used in the experimental investigation are explained in the following. Flow coefficient, ϕ, angle of attack, α, torque coefficient, C_T, pressure drop coefficient, ψ, and efficiency, η, are defined as :

$$\phi = \frac{V_a}{U} = \tan\alpha,$$
$$C_T = \frac{T}{\frac{1}{2}\rho\left(U^2 + {V_a}^2\right)AR_t},$$
$$\psi = \frac{\Delta P}{\frac{1}{2}\rho\left(U^2 + {V_a}^2\right)}, \quad (1)$$
$$\eta = \frac{C_T}{\psi\phi}$$

where the nomenclatures are U=blade speed of the tip, V_a=space average axial velocity, T=torque, ΔP=pressure drop across the blade, R_t=radius of the rotor, R_h=radius of the hub, annulus section area of $A = \pi\left({R_t}^2 - {R_h}^2\right)$, and ρ=air density. The Wells turbine operated with constant rotational speed has the unique characteristics that the torque is proportional to the square of the flow rate, and the pressure drop is proportional to the flow rate in the operation before stall.

Figures 4a ~ 4c show the torque coefficient, the pressure drop coefficient, and the efficiency of the Wells turbine with the rectangular blade, respectively. The stall angle is large, such as 18º because of the thick blade. Figure 5 shows the characteristics of the Wells turbines with the fan-shaped blades with the different sweep angles. The stall angles of the normal blade, the swept forward blade, and the swept back blade are 11.4º, 8º and 10º, respectively.

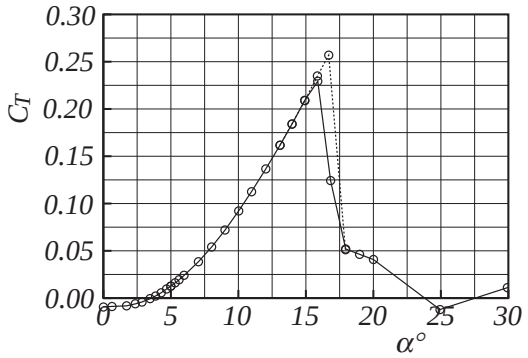

(a) Torque coefficient

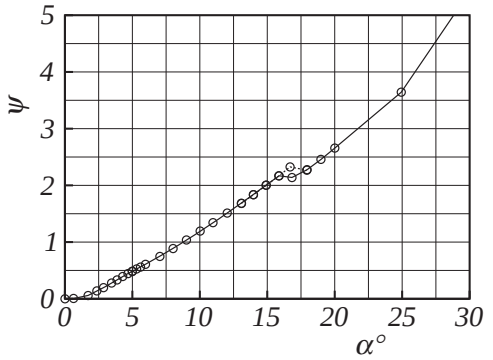

(b) Pressure drop coefficient

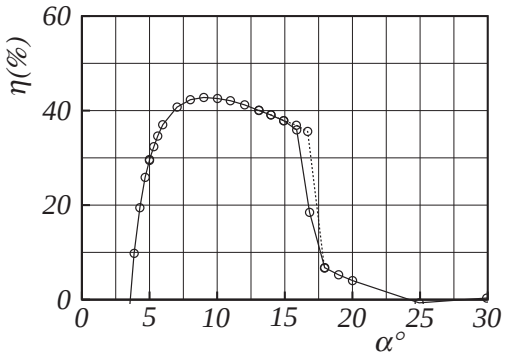

(c) Efficiency

Fig. 4 Characteristics of Wells turbine with rectangular blades

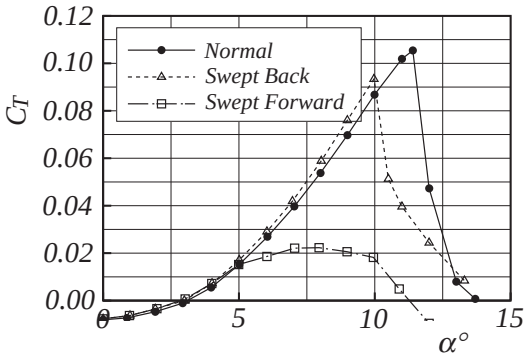

(a) Torque coefficient

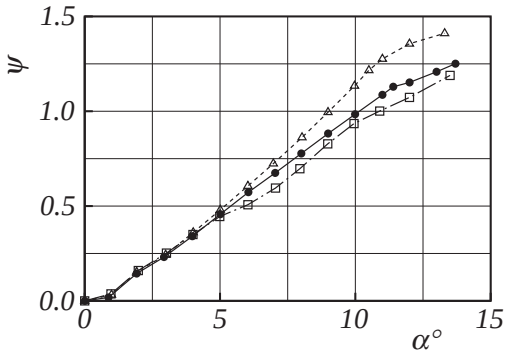

(b) Pressure drop coefficient

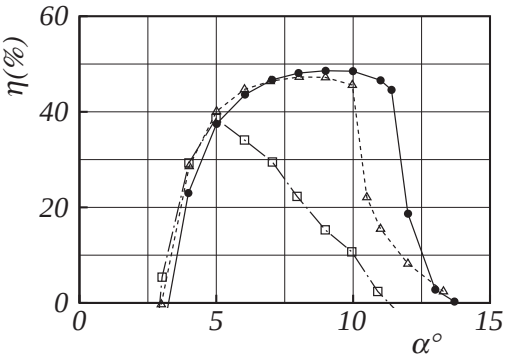

(c) Efficiency

Fig. 5 Characteristics of Wells turbine with fan-shaped blades

Figure 6 shows the axial velocity distributions at the inlet and the outlet, which are compared the rectangular blade to the fan-shaped blade. The velocity distribution of rectangular blade is flat at the inlet position and increases as the radius from the hub to the tip at the outlet position. On the other hand, the velocity distributions of the fan-shaped blade are flat from the hub to the tip at both inlet and outlet position.

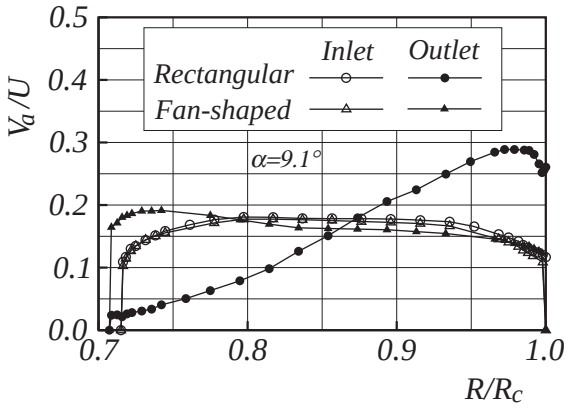

Fig. 6 Axial velocity distributions

3.2 Flows around the Blades

Figure 7 shows the flow patterns on the Wells turbine with the rectangular blade visualized with the oil-film method. Figure 7a shows the flow on the surface when the angle of attack is α=0º, Fig. 7b shows the flow on the suction surface whose angle of attack is α=15º just before the stall, and Fig. 7c shows the flow on the suction surface whose angle of attack is α=19º after the stall.

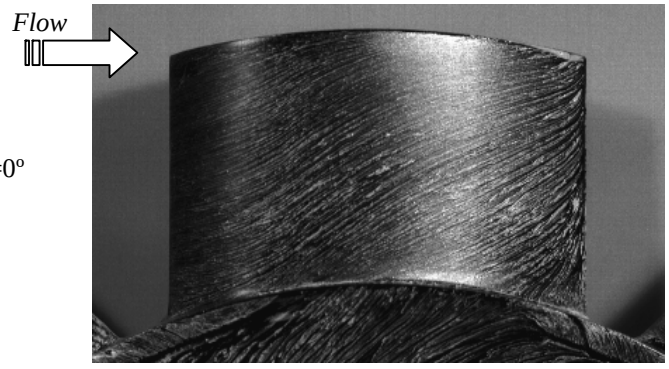

(a) α=0º

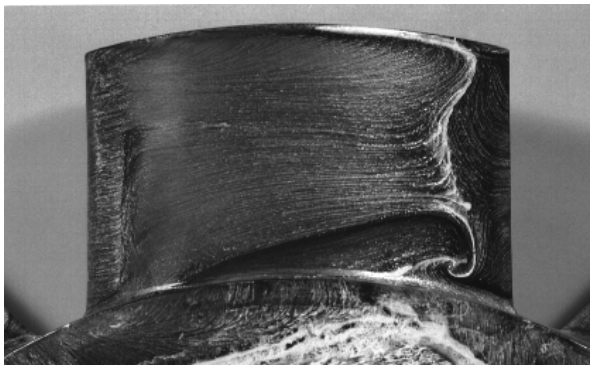

(b) α=15º

(c) α=19º

Fig. 7 Flow patterns on the suction surface of the rectangular blades

In Fig. 7a the oil streaks on the pressure sides form a pattern similar to a logarithmic spiral because of the centrifugal force. The figures for the other angles of attack show the same patterns on the pressure sides. In Fig. 7b, the pattern on the suction sides show that the fluid near the blade surface flows in the circumferential direction and the separation region on the blade is observed near the trailing edge. The separation near the trailing edge makes up the rectangular pattern, because the angle of attack is distributed uniformly from the hub to the tip by the axial velocity distribution of the rectangular blade in Fig. 6. What is most important in this oil pattern is the reverse flow, which initiate at the corner of the trailing edge and tip. This phenomenon manifests with a kind of an envelope line of oil streaks flowing in the upstream direction. It is supposed that this reverse flow shown with oil streaks triggers off to induce a large scale separation, which creates the counterclockwise swirl shown in Fig. 7c.

The authors have been very interested in the existence of the swirl, which has a clear eye in the oil-film pattern on the blade, and the reason for the flow patterns in the stall curling in the counterclockwise direction. The understanding and clarification of the creation mechanism of the swirl will be useful for improving the characteristics of the performance of Wells turbines.

Figures 8 ~ 10 show the flow patterns on the Wells turbine with the fan-shaped blades visualized with the oil-film method. Figure 8 shows the flow patterns on the normal blade at α=9º before the stall and α=15º after the stall, which has no sweep angle. Flow visualisation on a rotor with blades of several planforms indicates a large effect of the blade sweep on the boundary layer separation on the blades. The separation region near the trailing edge makes up the triangle pattern because the angle of attack at the hub is larger than at the tip owing to the flat axial velocity from the hub to the tip in Fig. 8.

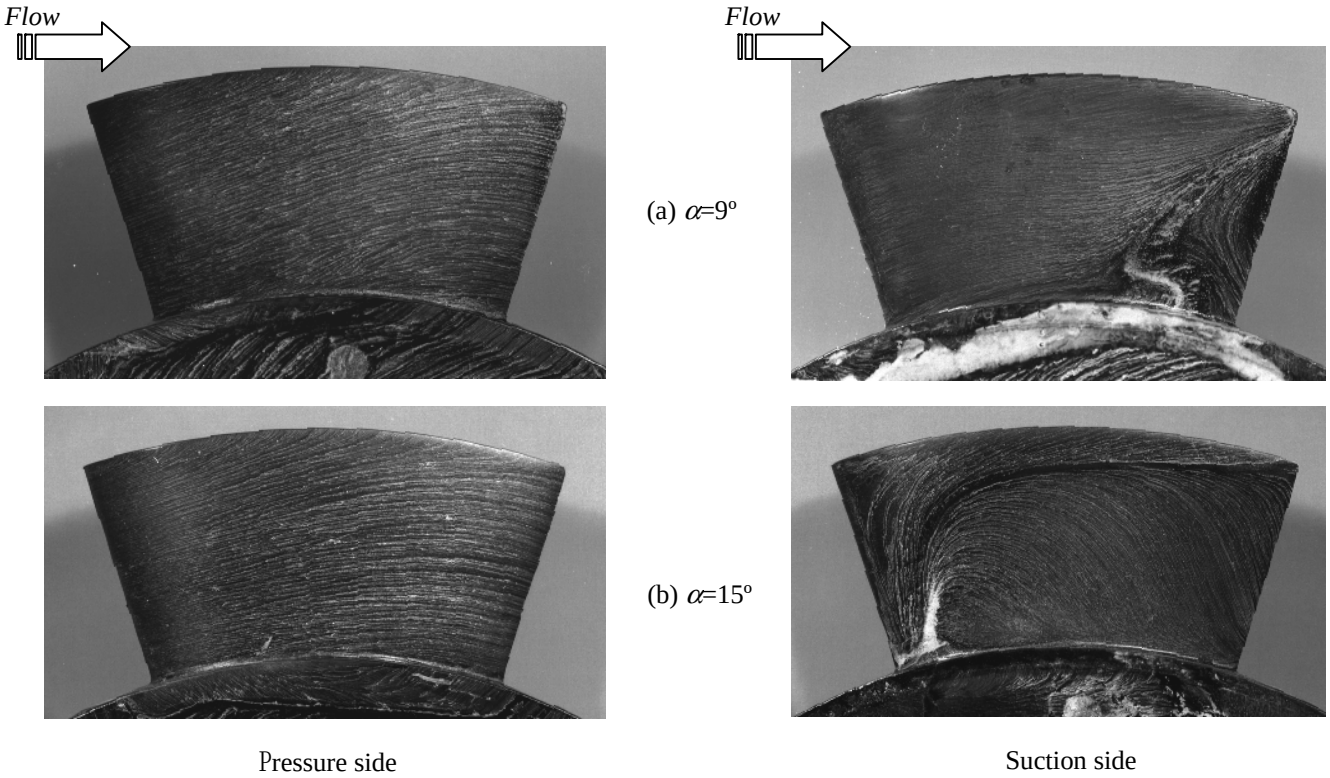

Fig. 8 Flow patterns on the fan-shaped and normal blades

Figure 9 shows the flow patterns on the swept forward blade at α=6.8º of the stall and α=9º after the stall. The flow patterns on the blade have the larger separation regions than on the normal blade at the trailing edge. Fig. 10 shows the flow patterns on the swept back blade at α=9º. The flow patterns on the blade have the smaller separation regions than on the normal blade and the swept back blade at the trailing edge. Therefore the efficiency is improved at the angle of attack less than 7 degrees such as shown as Fig. 5c. But the stall angle is 10º, and smaller than the normal blade.

4. Conclusion

The Wells turbine produces a complicated flow field due to the peculiar arrangement of blades, which can rotate in the same direction irrespective of the oscillating airflow. In order to understand these flows, flow visualization is carried out with an oil-film method in the water tunnel. Very interesting and complex flow patterns are observed especially in the flow of large angle of attack. The phenomena cleared by this paper are as follows:

(1) The flow on the pressure sides forms a pattern similar to a logarithmic spiral because of the centrifugal force.
(2) The separation patterns near the trailing edge are rectangular on the rectangular blade and triangle on the fan-shaped blade. The reason is the different distributions of angle of attack which occur from the different axial velocity distributions at the outlet. The axial velocity distributions increase as the radius of blade for the rectangular blade and become uniformly for the fan-shaped blade, because of the different spacing between the blades.
(3) It is found that the large scale separation is induced and the counterclockwise vortex on the blade is produced when the turbine stalls.

(4) The performances of the swept forward blade are inferior to the other ones, because the flow around the hub separates even the small angle of attack, 6.5º.
(5) The flow patterns on the blade have the smaller separation regions at the trailing edge than on the normal blade and the swept forward blade. Therefore the efficiency is improved at the angle of attack less than 7 degrees. But the stall angle, 10º, is smaller than the normal blade.

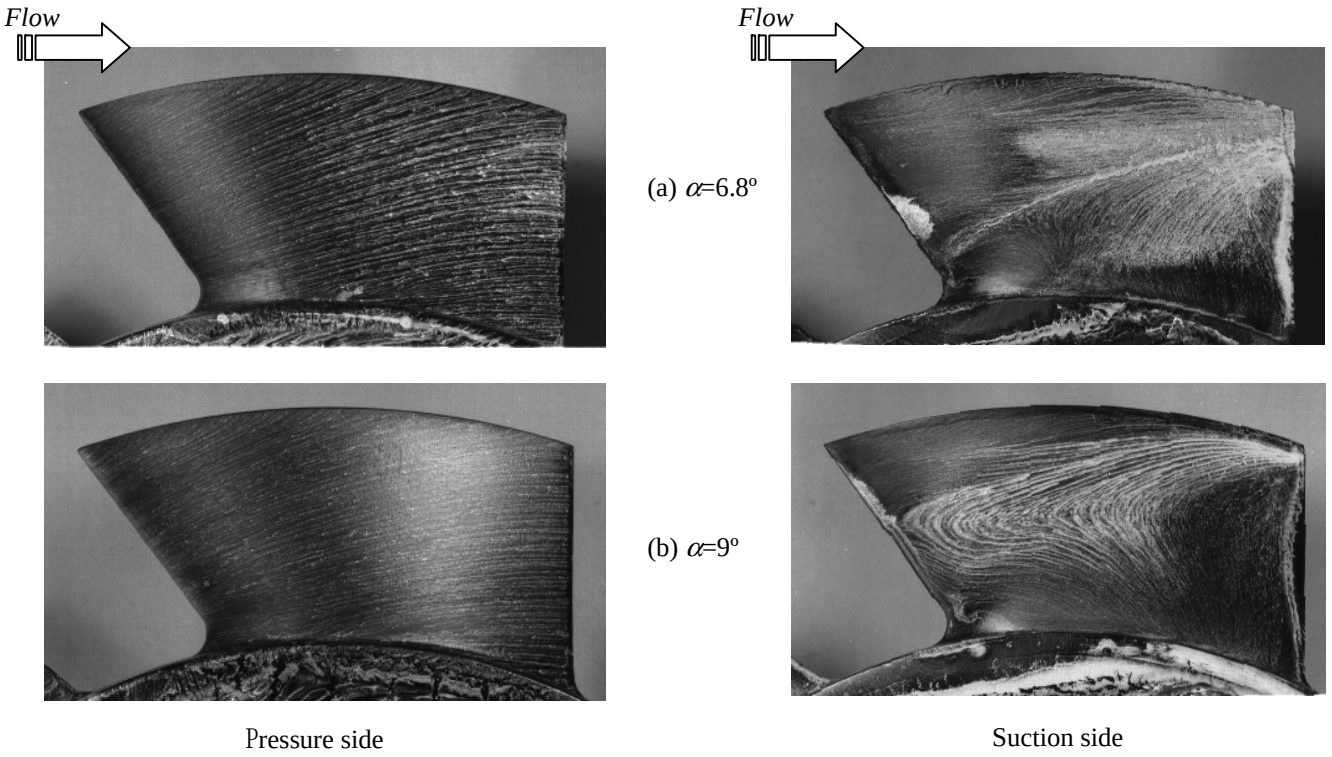

Fig. 9 Flow patterns on the fan-shaped and swept forward blades

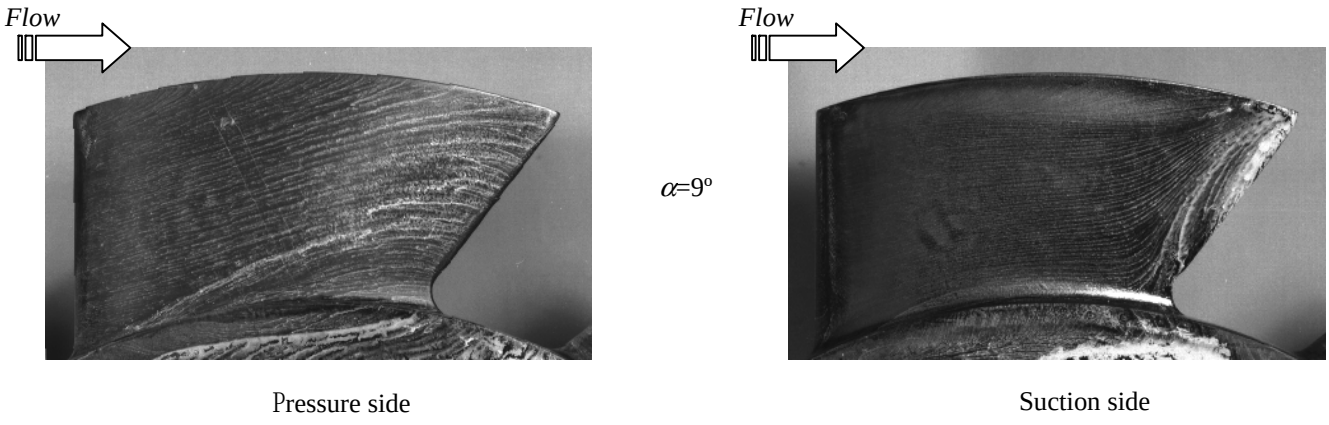

Fig. 10 Flow patterns on the fan-shaped and swept back blades

References

[1] Hotta, H.; Miyazaki, T. Washio, Y.; Ishii, S., 1988, "On the Performance of the Wave Power Device Kaimei the results on the open sea tests," Proceedings of the Seventh International Conference on Offshore Mechanics and Arctic Engineering, ASME, pp. 91-96.
[2] Washio, Y.; Osawa, H.; Nagata, E.; Furuyama, H.; Fujia, T., 2000, "The Offshore Floating Type Wave Power Device "Mighty Whale": Open Sea Tests," Proceedings of 10th International Offshore and Polar Engineering Conference, Seattle, ISOPE, pp. 373-380.
[3] Suzuki, M.; Arakawa, C., 2000, "Guide Vanes Effect of Wells Turbine for Wave Power Generator," International Journal of Offshore and Polar Engineering, ISOPE, Vol. 10, No. 2, pp. 153-159.
[4] Raghunathan, S., 1995, "The Wells Air Turbine for Wave Energy Conversion," Prog. Aerospace Sci., Vol. 31, pp. 335-386.
[5] Raghunathan, S., Setoguchi, T., Kaneko, K., 1989, "Some Techniques to Improve the Operation Range of the Wells Turbine for Wave Power Generator," JSME International Journal, Series II, Vol. 32, No. 1, pp. 71-77.
[6] Gato, L.M.C., Falcao, A.F. de O., 1990, "Performance of the Wells Turbine with a Double Row of Guide Vanes," JSME International Journal, Ser. II, Vol. 33, No. 2, pp. 265-271.
[7] Watterson, J.K., Raghunathan, S., 1997, "Computed Effects of Solidity on Wells Turbine Performance," JSME International

Conference on Fluid Engineering, pp. 833-838.
[8] Suzuki, M., Arakawa, C., 2001, “Numerical Simulation of 3-D Stall Mechanism on Wells Turbine for Wave-Power Generating System, International Journal of Offshore and Polar Engineering, ISOPE, Vol. 11, No. 4, pp. 315-320.